Energy 51 (2013) 314–322

Contents lists available at SciVerse ScienceDirect

Energy

journal homepage: www.elsevier.com/locate/energy

Mathematical modeling of solar chimney power plants

Atit Koonsrisuk*, Tawit Chitsomboon [1]

School of Mechanical Engineering, Institute of Engineering, Suranaree University of Technology, Muang District, Nakhon Ratchasima 30000, Thailand

ARTICLE INFO

Article history:
Received 27 August 2012
Received in revised form
9 October 2012
Accepted 10 October 2012
Available online 13 November 2012

Keywords:
Solar chimney power plant
Mathematical model
Solar energy
Natural convection
Dimensional analysis

ABSTRACT

The solar chimney power plant is a system with promise to generate electrical power from free solar energy. In this study, a solar collector, chimney and turbine are modeled together theoretically, and the iteration techniques are carried out to solve the resulting mathematical model. Results are validated by measurements from an actual physical plant. Moreover, the model is employed to predict the performance characteristics of large-scale commercial solar chimneys, indicating that the plant size, the factor of pressure drop at the turbine, and solar heat flux are important parameters for performance enhancement. In addition, the study proposes that the most suitable plant, affordable by local government standards to respond to the electricity demand of a typical village in Thailand, is the one with a collector radius and chimney height of 200 m and 400 m, respectively. Furthermore, it is shown that the optimum ratio between the turbine extraction pressure and the available driving pressure for the proposed plant is approximately 0.84. A simple method to evaluate the turbine power output for solar chimney systems is also proposed in the study using dimensional analysis.

1. Introduction

The solar chimney power plant is a solar electricity production facility, which uses solar radiation to increase the internal energy of air flowing through the system. The schematic of a typical solar chimney is sketched in Fig. 1. In this plant, air is heated as a result of the greenhouse effect under a translucent roof (collector). As the roof is open at its periphery, buoyancy drives a continuous flow from the roof perimeter into the chimney located at the middle of the roof. An electricity-generating turbine is set in the path of the air current to convert the kinetic energy of the flowing air into electricity.

Solar chimney power plants can convert only a small portion of the collected solar energy into electricity, but they make up for this disadvantage by their economical, robust construction and low maintenance costs [1]. Economic viability requires the optimum configurations of each component. Efficient conversion of fluid power to shaft power depends primarily on the turbine operation. During the day, mass flow through a system changes, due mainly to the variation of solar radiation. Accordingly, the turbine blade pitch should be adjusted during its operation to regulate the power output. In this study, the optimal operating conditions of the turbine unit are determined in consideration of the plant power output.

To evaluate the available plant power output, researchers defined the ratio of the pressure drop across the turbine to the total available driving pressure of a system, which is symbolized as p_{turb}/p_{tot} herein. Indeed, most investigators have assumed that the optimum p_{turb}/p_{tot} is 2/3 ([1–8]). Although the computations of values taken from Ref. [1] showed that p_{turb}/p_{tot} used is 0.82, Ref. [9] illustrated that the ratio is between 0.66 and 0.7 during the day. Furthermore Von Backström and Fluri [10], stated without reference that the optimum ratio is 0.8. Additionally Nizetic and Klarin, Schlaich et al. [11,12], proposed analytical approaches, and showed that the pressure ratio varied in the range of 0.8–0.9. Meanwhile Bernardes et al. [13] reported an optimum value of 0.97. Although the turbine under consideration is encased by a tower, some authors use the ratio as 16/27 ([14–16]), which is the Betz limit obtained for an actuator disc in a free stream situation.

We develop a detailed theoretical model here to evaluate the performance of solar chimney power systems. Our paper also presents the operating range of the turbine. It tries to determine how to maximize the fluid power by adjusting the pressure drop across the turbine and the flow through it.

2. Optimal pressure ratio

According to the operation principle mentioned above, the air inside a system is less dense than the atmospheric air outside. The air moves in and out of the solar chimney system continuously, driven by the pressure difference between the inside and outside.

* Corresponding author. Tel.: +66 44 224515; fax: +66 44 224613.
E-mail addresses: atit@sut.ac.th (A. Koonsrisuk), tabon@sut.ac.th (T. Chitsomboon).
[1] Tel.: +66 44 224515; fax: +66 44 224613.

0360-5442/$ – see front matter © 2012 Elsevier Ltd. All rights reserved.
http://dx.doi.org/10.1016/j.energy.2012.10.038

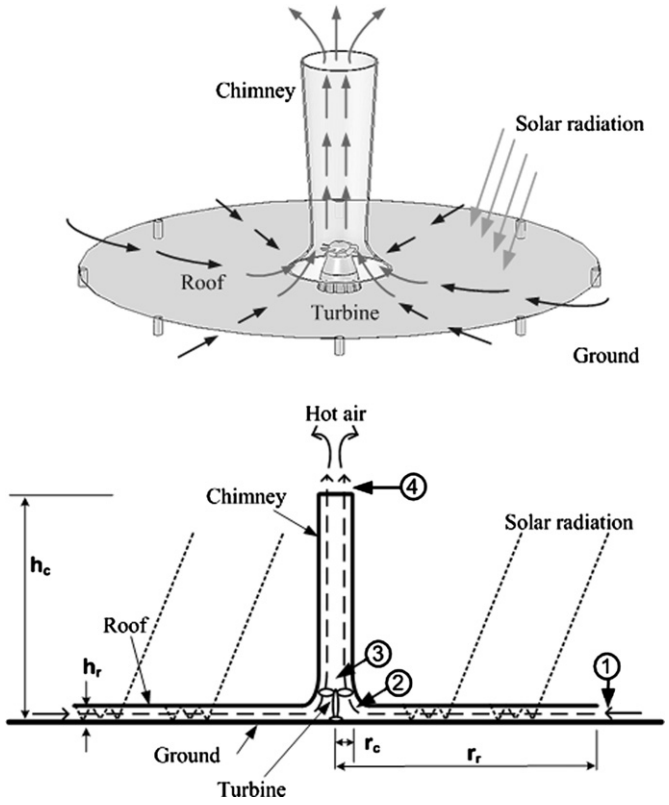

Fig. 1. Schematic layout of solar chimney power plant.

This pressure difference will be called the *available driving pressure* and symbolized as Δp_{tot}. Neglecting friction losses [17], Δp_{tot} can be subdivided into a turbine extraction component representing the pressure extracted at the turbine, and a dynamic component describing the kinetic energy of the airflow:

$$\Delta p_{tot} = \Delta p_{turb} + \Delta p_{dyn}. \quad (1)$$

Let us define the ratio p_{turb}/p_{tot} as x, so that

$$\Delta p_{turb} = x\Delta p_{tot}. \quad (2)$$

Using the standard definition for dynamic pressure, we obtain

$$\Delta p_{dyn} = \frac{1}{2}\rho_c V^2_{with\ turb} \quad (3)$$

Without the turbine, the maximum flow speed is achieved and the whole driving potential is used to accelerate the flow, so that

$$\Delta p_{tot} = \frac{1}{2}\rho_c V^2_{no\ turb}. \quad (4)$$

Substituting Eqs. (2)–(4) into Eq. (1) yields,

$$V_{with\ turb} = V_{no\ turb}\sqrt{(1-x)}. \quad (5)$$

The theoretical power extracted by the turbine can be determined from the energy equation and Gibbs relation from classical thermodynamics:

$$\dot{W}_{ext} = \dot{m}\int v\mathrm{d}p \approx \frac{\dot{m}}{\rho_{turb}}\Delta p_{turb}. \quad (6)$$

Substituting Eqs. (2) and (5) into Eq. (6) and using $\dot{m} = \rho_{turb}A_C V_{with\ turb}$, we obtain:

$$\dot{W}_{ext} = A_c \cdot \sqrt{1-x} \cdot V_{no\ turb} \cdot x \cdot \Delta p_{tot}. \quad (7)$$

The optimal x for the maximum power extraction can be obtained by assuming that $V_{no\ turb}$ and Δp_{tot} are not functions of x and solving $\partial \dot{W}_{ext}/\partial x = 0$. The result for the optimal pressure ratio is

$$x_{opt} = \frac{2}{3} \quad (8)$$

Consequently, maximum power is obtained when the turbine extraction pressure is 2/3 of the available driving pressure, corresponding to the value that most researchers have utilized. Using our assumptions, the optimal pressure ratio of 2/3 is valid only for the constant-driving-pressure systems (i.e. for the constant air temperature increase).

Equation (7) shows that the plant power output can be increased by adjusting the turbine extraction pressure. Later, it will be shown that changing x affects $\dot{m}$, $\dot{W}_{ext}$, and Δp_{tot}. As a result, the

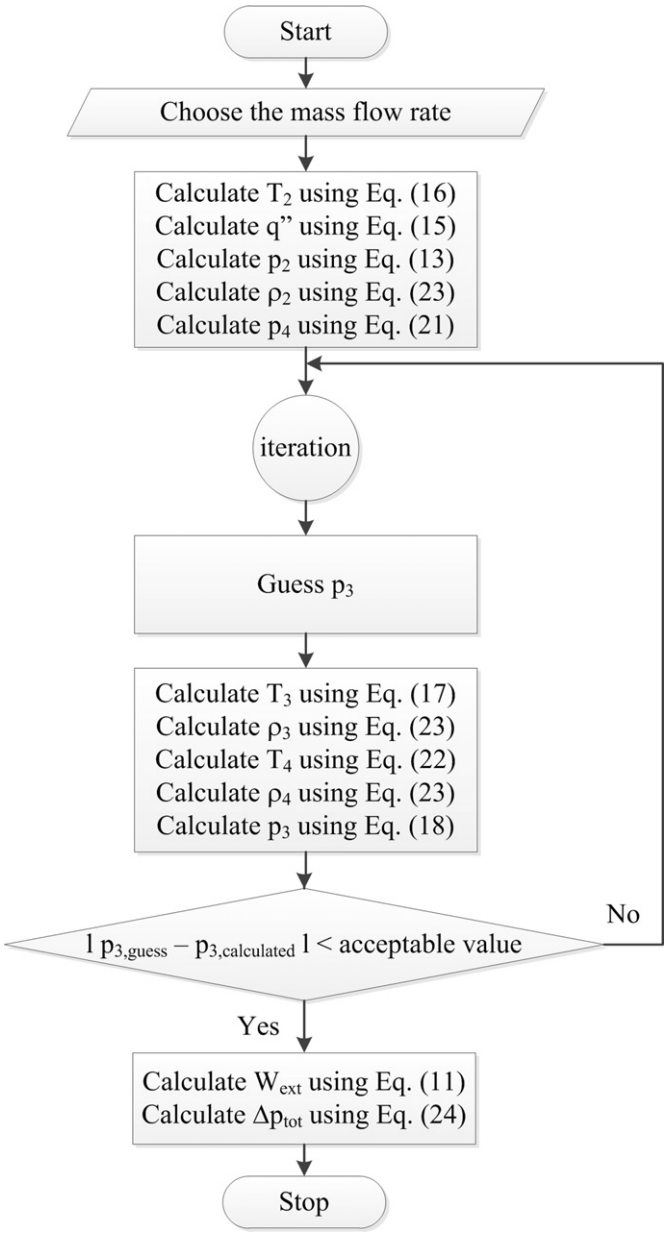

Fig. 2. Flowchart of solution procedures.

Table 1
Geometrical dimensions of the pilot plant in Manzanares, Spain.

Mean roof radius, r_r	122 m
Average roof height, h_r	1.85 m
Tower height, h_c	194.6 m
Tower radius, r_c	5.08 m

assumption that Δp_{tot} is not the function of x would render inaccurate the predicted power.

3. The mathematical model

With the stations numbered as in Fig. 1, the temperature rise can be estimated from the energy equation across the roof portion:

$$\dot{m}c_p(T_2 - T_1) + \frac{1}{2}\dot{m}\left(V_2^2 - V_1^2\right) = q''A_r \tag{9}$$

For simplicity, frictional effect is ignored since the velocity in this region is quite low. Because the flow is in the very low Mach number regime, the kinetic energy contribution can be safely neglected, therefore,

$$\dot{m}c_p\Delta T = q''A_r. \tag{10}$$

When the inlet solar radiation is assumed constant, Eq. (10) shows that the temperature rise is inversely proportional to the mass flow rate.

In this analysis, the turbine is treated as the Rankine–Froude actuator disc. The assumptions on which this actuator disc based are listed as follows [18]:

1. Steady, homogeneous wind.
2. Uniform flow velocity at disc.
3. Static pressure decreases discontinuously across the disc.
4. No rotation of flow produced by disc.

Accordingly, Eq. (6) becomes,

$$\dot{W}_{ext} = \frac{\dot{m}}{(\rho_2 + \rho_3)/2}(p_2 - p_3). \tag{11}$$

By synthesizing equations for continuity, momentum and energy of the flow under the roof Chitsomboon [19], proposed that

$$p_2 - p_1 = \int_1^2 \frac{\rho V^2}{(1 - M^2)}\left(\frac{dA}{A} - \frac{q''dA_r}{\dot{m}c_pT}\right). \tag{12}$$

Assuming that q'', c_p and $\dot{m}$ are constant, ρ and T can be approximated to be ρ_1 and T_1 without significantly affecting the numerical values of the terms. The Mach number is again assumed to be very low and thus can be neglected; the equation is then simplified to be,

Table 2
Comparison between measured data from Manzanares pilot plant and theoretical results. (data on 2nd September 1982 taken from Ref. [23]).

Time		10.00	12.00	14.00	16.00
I (W/m^2)		744.4	850	755.6	455.6
η_{coll} (%)		24.3	27.1	25.7	23.6
T_1 (°C)		21.1	23.4	26.1	27.9
ΔT_{12} (°C)		14.8	17.8	17.4	11.3
V_4 (m/s)	Measured	7	9	7	7.7
	Theory	6.72	7.25	6.29	5.28
Δp_{turb} (mbar)	Measured	0.8	0.8	0.84	0.6
	Theory	0.62	0.74	0.81	0.51

Table 3
Data of Manzanares pilot plant for 1st September 1989 taken from Ref. [24].

Global solar radiation (W/m^2), I	1017
Ambient temperature (°C), T_1	18.5
Ambient pressure (Pa), p_1	92,930
Collector absorption coefficient, α	0.65
Collector loss coefficient (W/m^2 K), U	15
Turbine efficiency	0.85
Generator and gearbox efficiency	0.9
Upwind velocity (m/s), V_4	8.1

$$p_2 = p_1 + \frac{\dot{m}q''}{2\pi h_r^2\rho_1 c_p T_1}\ln\frac{r_r}{r_c} - \frac{\dot{m}^2}{2\rho_1}\left(\frac{1}{A_2^2} - \frac{1}{A_1^2}\right) \tag{13}$$

where p_1, ρ_1 and T_1 are approximated as p_∞, ρ_∞ and T_∞, respectively. Eq. (13) shows that p_2 is the combination of the inlet pressure, p_1, with the pressure increase due to heat addition, $(\dot{m}q''/2\pi h_r^2\rho_1 c_p T_1)\ln r_r/r_c$, and the pressure decrease due to flow area reduction towards the center of the roof, $\dot{m}^2/2\rho_1(1/A_2^2 - 1/A_1^2)$. Order of magnitude analysis reveals that $\dot{m}^2/2\rho_1(1/A_2^2 - 1/A_1^2)$ is significantly greater than $(\dot{m}q''/2\pi h_r^2\rho_1 c_p T_1)\ln r_r/r_c$.

Rearranging Eq. (10) yields

$$T_2 = T_1 + \frac{q''A_r}{\dot{m}c_p} \tag{14}$$

where, according to Ref. [20],

$$q'' = \alpha\cdot I - U\cdot\Delta T. \tag{15}$$

It should be noted that ΔT in Eq. (15) is the temperature difference between the air inside and outside a solar collector which is assumed here to be equal to $(T_2 - T_1)$.

Accordingly,

$$\Delta T = \frac{\alpha\cdot I}{\dot{m}\cdot c_p/A_r + U}. \tag{16}$$

If the work extraction process at the turbine is assumed to be an isentropic process, then

$$T_3 = T_2\left(\frac{p_3}{p_2}\right)^{\frac{\gamma-1}{\gamma}}. \tag{17}$$

Furthermore, by rearranging the momentum and continuity equations for the flow through a constant area vertical tower of height, h_c, we obtain

$$p_3 = p_4 + \frac{1}{2}(\rho_3 + \rho_4)\cdot g\cdot h_c + \left(\frac{\dot{m}}{A_c}\right)^2\left(\frac{1}{\rho_4} - \frac{1}{\rho_3}\right). \tag{18}$$

If we consider the atmospheric air outside the solar chimney system, the hydrostatic equilibrium requires that

$$\frac{dp}{dz} = -\rho g. \tag{19}$$

According to Ref. [21], when the atmospheric air parcel is regarded as an unsaturated medium and expands slowly to a lower

Table 4
Comparison between measured data from Manzanares pilot plant and theoretical results (data on 1st September 1989).

Parameter	Measured	Theory
T_2 (°C)	38	41.5
$\dot{W}_{ext}$ (kW)	48.4	48.3

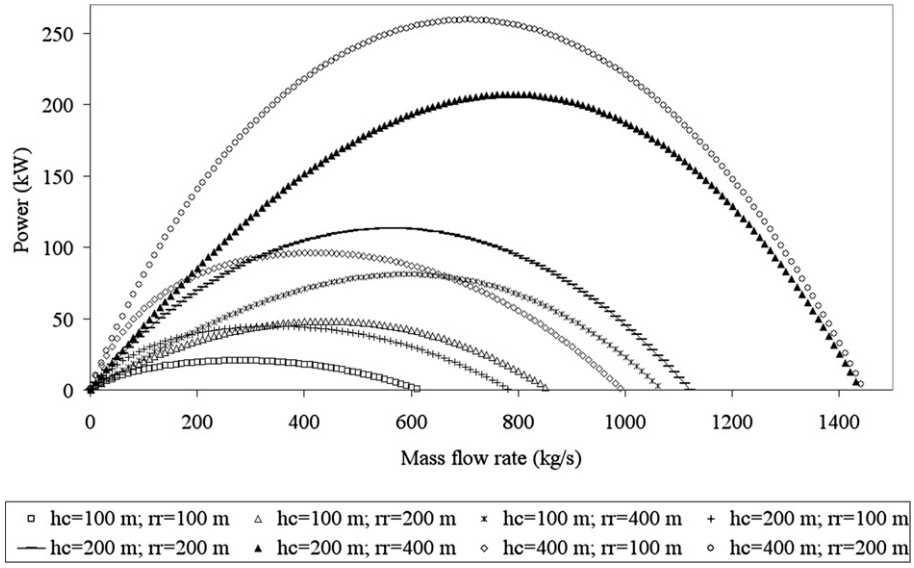

Fig. 3. Influence of mass flow rate on power output for solar irradiation = 600 W/m^2. (h_r = 2 m and r_c = 4 m for all plants).

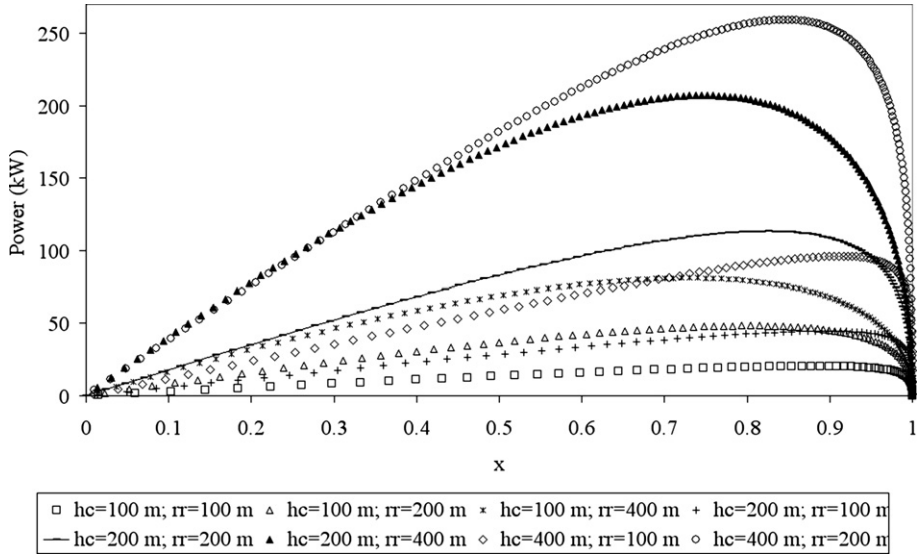

Fig. 4. Influence of pressure ratio (cf. Eq. (2)) on power output for solar irradiation = 600 W/m^2. (h_r = 2 m and r_c = 4 m for all plants).

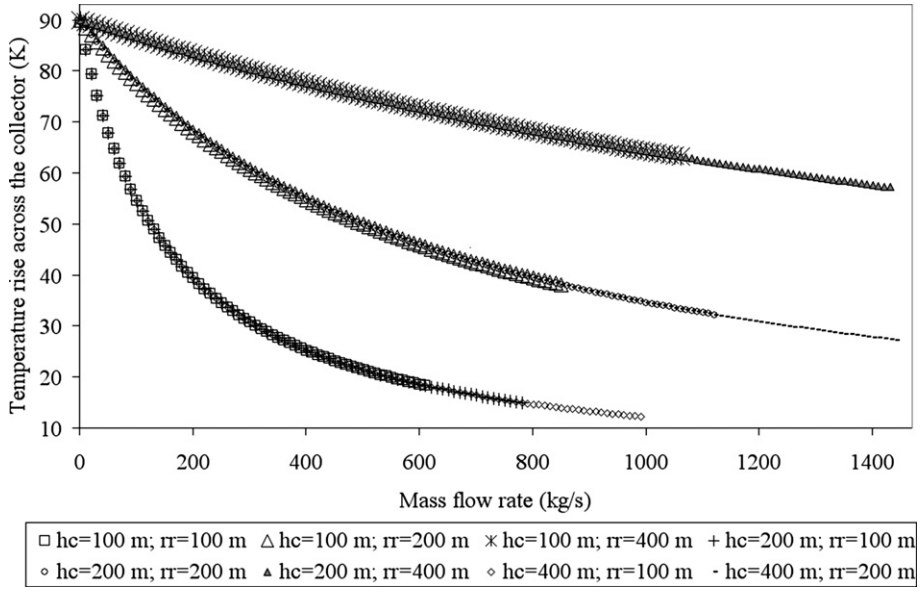

Fig. 5. Influence of mass flow rate on collector temperature rise for solar irradiation = 600 W/m^2. (h_r = 2 m and r_c = 4 m for all plants).

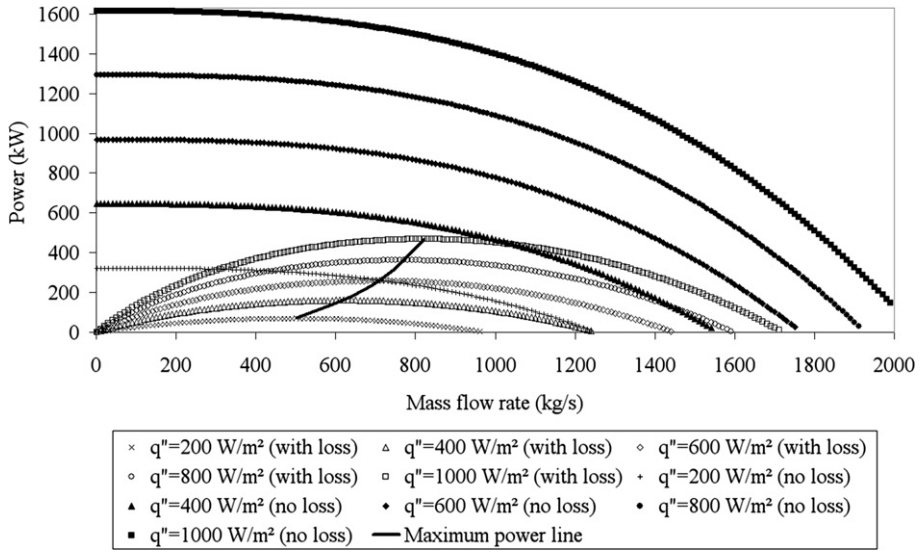

Fig. 6. Influence of mass flow rate on power output along lines of constant solar irradiation. ($h_r = 2$ m, $r_r = 200$ m, $h_c = 400$ m and $r_c = 4$ m for all cases).

atmospheric pressure without exchange of heat, the dry adiabatic temperature lapse rate equation can be written as

$$T = T_\infty - \frac{g}{c_p} z. \tag{20}$$

Assuming that the air obeys the ideal gas equation of state, Eq. (20) can be substituted into Eq. (19) to give p_4 for the outside air as

$$p_4 = p_\infty \left(1 - \frac{g}{c_p T_\infty} h_c\right)^{\frac{c_p}{R}}. \tag{21}$$

Consider that a dry adiabatic lapse rate can be applied to the flow in a tower. In accordance with Eq. (20),

$$T_4 = T_3 - \frac{g}{c_p} h_c. \tag{22}$$

For an ideal gas,

$$\rho_2 = \frac{p_2}{RT_2}, \quad \rho_3 = \frac{p_3}{RT_3}, \quad \rho_4 = \frac{p_4}{RT_4}. \tag{23}$$

Theoretically the driving pressure of the solar chimney (Δp_{tot}) is the difference between pressure potentials caused by the column of cold air outside the chimney and the corresponding column of warm air inside the chimney [22]. Consider that the pressure at the chimney exit and the pressure outside the chimney but at the same height as the chimney exit are approximately equal. Consequently, in this analysis we propose

$$\Delta p_{tot} = p_1 - p_3. \tag{24}$$

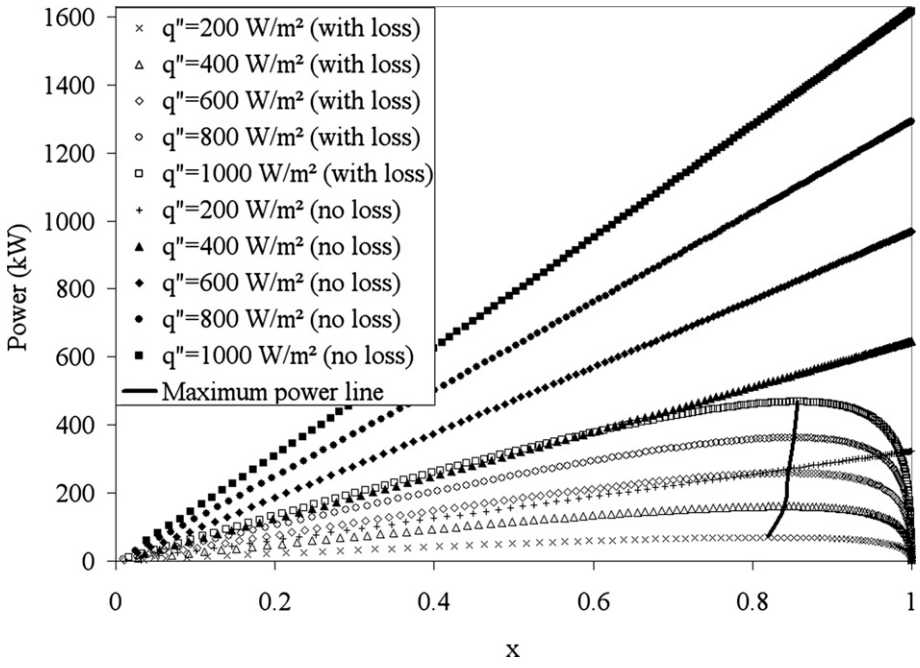

Fig. 7. Influence of pressure ratio on power output along lines of constant solar irradiation. ($h_r = 2$ m, $r_r = 200$ m, $h_c = 400$ m and $r_c = 4$ m for all cases).

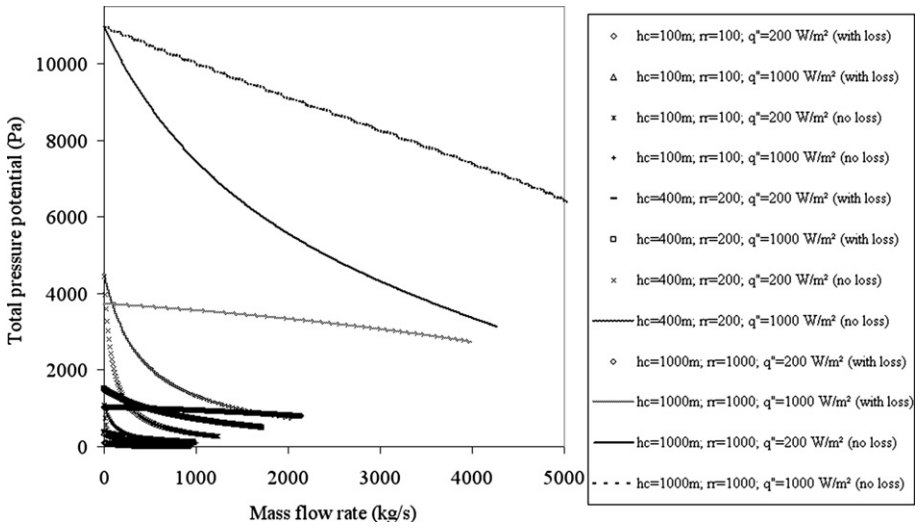

Fig. 8. Influence of mass flow rate on available driving pressure along lines of constant solar irradiation. ($h_r = 2$ m and $r_c = 4$ m for all plants).

One can argue that this way of definition makes Δp_{tot} insensitive to the chimney height. Numerical simulation of several different plant sizes, on the other hand, showed that Δp_{tot}, calculated by using Eq. (24), is a function of the chimney height.

4. Solution procedure

According to the formulation above, if the mass flow rate is known or assumed then the power output can be attained. The steps of calculating the plant power output are:

1. Choose the mass flow rate,
2. Calculate T_2 using Eq. (16),
3. Calculate q'' using Eq. (15),
4. Calculate p_2 using Eq. (13),
5. Calculate p_2 using Eq. (23),
6. Calculate p_4 using Eq. (21),
7. Guess p_3, then calculate T_3, ρ_3, T_4, ρ_4 using Eq. (17), Eq. (23), Eq. (22) and Eq. (23), respectively. Calculate p_3 using Eq. (18), then compare the new p_3 to the former p_3. Perform the iteration process until the difference between corresponding new and old p_3 is less than an acceptable value.
8. Calculate $\dot{W}_{ext}$ using Eq. (11),
9. Calculate Δp_{tot} using Eq. (24).

A flowchart for these procedures is illustrated in Fig. 2.

5. Results and discussion

5.1. Validation of the model with experimental data

To validate the analytical model, our theoretical data was compared with the experimental results of the prototype from Manzanares, Spain. The plant dimensions are given in Table 1.

The measured data on September 2nd, 1982 are adopted from Ref. [23]. The comparisons between the theoretical predictions and the experimental values are presented in Table 2. Based on the data provided by the reference article, instead of using Eq. (15), q'' was computed from

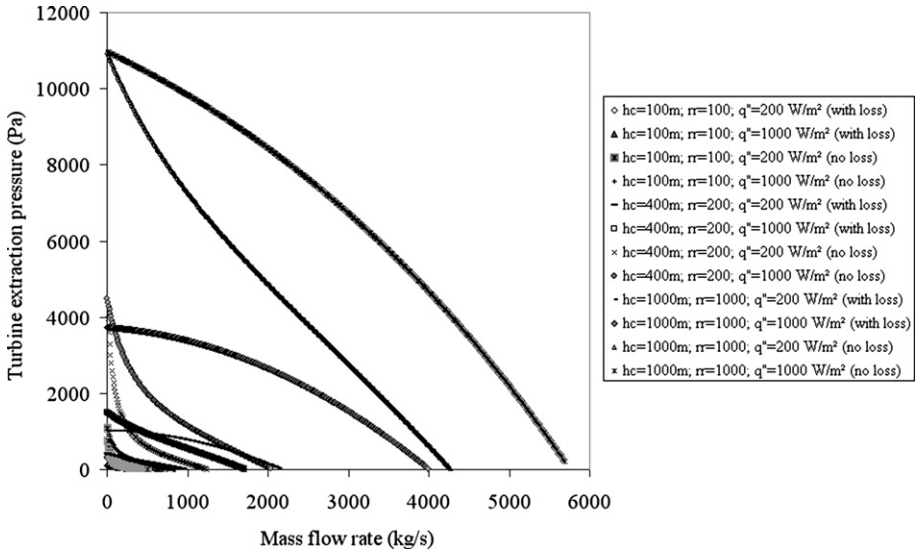

Fig. 9. Influence of mass flow rate on turbine extraction pressure along lines of constant solar irradiation. ($h_r = 2$ m and $r_c = 4$ m for all plants).

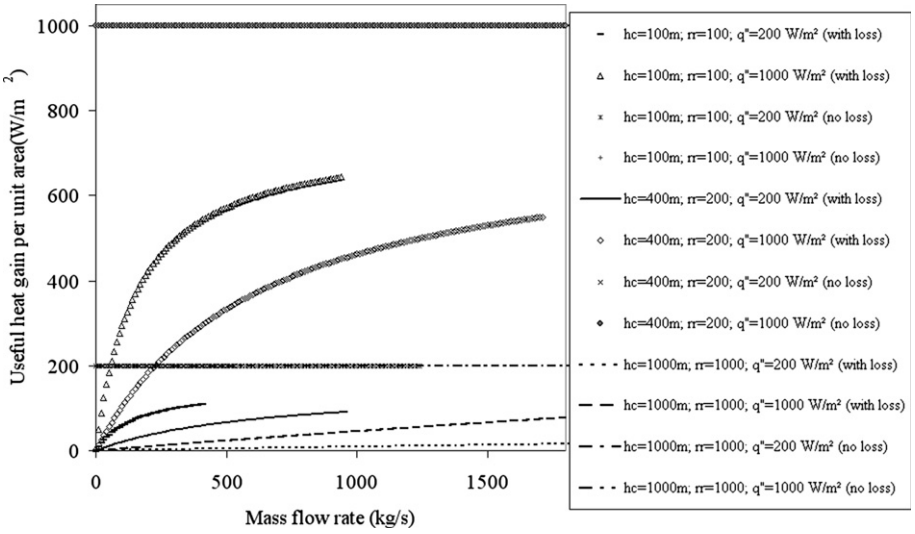

Fig. 10. Influence of mass flow rate on useful heat gain extracted from the collector along lines of constant solar irradiation. ($h_r = 2$ m and $r_c = 4$ m for all plants).

$$q'' = \eta_{coll} \cdot I \tag{25}$$

where η_{coll} is the collector efficiency (defined as in Eq. (26)). The values of I, η_{coll}, T_1, ΔT_{12}, V_4 (measured) and Δp_{turb} (measured) displayed in Table 2 are taken from Ref. [23]. It is clear that all the predicted values are underestimated in Table 2. This is consistent with the "conservative approximation" of p_2 as stated in Ref. [19]. The acceptable agreement between experimental and theoretical results for V_4 and Δp_{turb} can be clearly seen for the whole range of I.

Furthermore, the measured data from Manzanares prototype plant on September 1st, 1989 are taken from Ref. [24]. The data adopted are presented in Table 3. The comparisons shown in Table 4 indicate good agreement between theoretical and experimental results, which should support the reliability of the proposed models.

5.2. Performance characteristics of solar chimney systems

Eight plant sizes are examined and presented their characteristics in Figs. 3–5. Based on the cost model presented in Ref. [1], these plant dimensions are chosen such that the plant can be affordable by the local government of villages in Thailand. Figs. 3,4 show the calculated power output as a function of the mass flow rate and $\Delta p_{turb}/\Delta p_{tot}$. The parameters $\alpha = 0.75$ and $U = 5$ W/m^2 K for Eq. (15) are taken from Ref. [1]. The temperature rise across the collector is presented in Fig. 5. It is observed that for a specified mass flow rate, the temperature rise is a function of roof radius *only*: it does not depend on the chimney height, a consequence of the specified conditions and the mathematical model defined by Eq. (14). Thus it should not be construed that the temperature rise is actually not a function of the chimney height. It should also be noted that the designed solar heat flux in Figs. 3–5 is 600 W/m^2.

According to the total maximum demand of electricity and the number of electrified villages in Thailand reported by the Provincial Electricity Authority of Thailand [25], the power demanded by each village is approximately 200 kW. So the appropriate plant, which has a reasonable temperature rise of 20 K (see Fig. 5) and can serve the electricity demand for each village in Thailand (see Fig. 3), is one with a collector radius of 200 m and a chimney height of 400 m. From now on, any observations will be for this plant size.

The variations of the power as a function of the solar heat flux are shown in Figs. 6,7. In these figures, 'q″ (with loss)' refers to the systems that the solar heat fluxes were computed from Eq. (15). The name implies that only some part of the solar radiation was absorbed by the systems. On the other hand, 'q″ (no loss)' in the figures represents systems that absorb solar radiation completely which means the collector efficiency equals 100%. It can be seen that the maximum power of systems with loss occur somewhere between the maximum and minimum mass flow rate while the maximum powers for the systems without heat loss occur at the point that offers the minimum mass flow rate. Apparently the optimum pressure ratio depends on the magnitude of the solar heat flux as displayed in Fig. 7. It is not equal to 2/3, but is approximately 0.84.

To investigate further the effect of the plant size on the flow characteristics, Figs. 8–10 show the relationships between Δp_{13}, Δp_{23}, q″ and $\dot{m}$ for plants with different sizes. It is clear that their relations depend on the plant sizes. Fig. 11 shows the collector efficiency that is defined as

$$\eta_{col} = \dot{m} c_p \Delta T_{12} / q'' A_r \tag{26}$$

It is apparent in the figure that the collector efficiency is not a function of the solar heat gain, but depends on the plant size, so

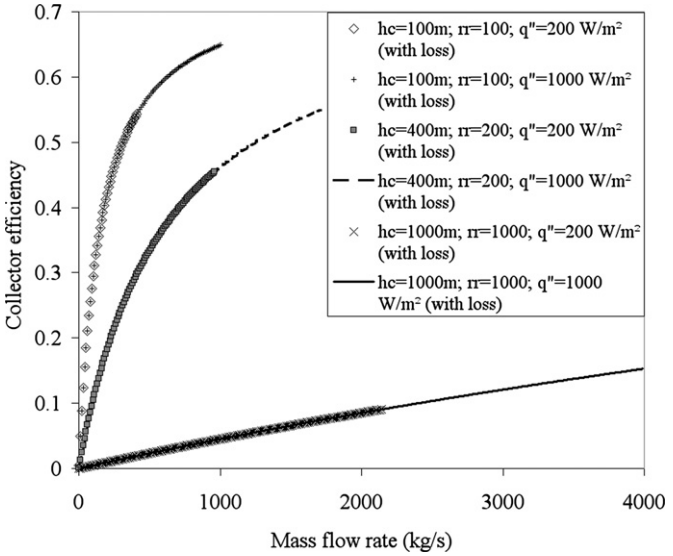

Fig. 11. Influence of mass flow rate on collector efficiency (cf. Eq. (26)) along lines of constant solar irradiation. ($h_r = 2$ m and $r_c = 4$ m for all plants).

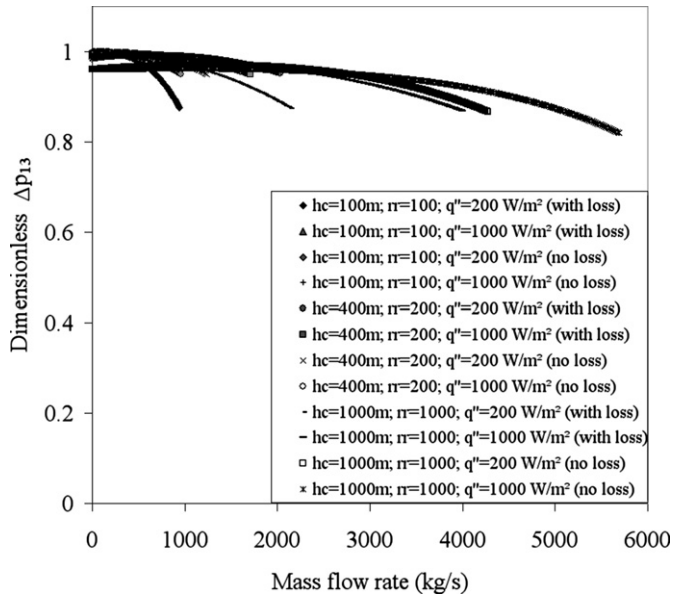

Fig. 12. Influence of mass flow rate on dimensionless Δp_{13} (cf. Eq. (29)) along lines of constant solar irradiation. ($h_r = 2$ m and $r_c = 4$ m for all plants).

that there is no representative value. We observe that the efficiency decreases as the collector size increases, explainable by the fact that when the plant size increases, the temperature rise across the collector increases as depicted in Fig. 5 and the solar heat gain decreases subsequently as defined by Eq. (15). Thus the collector efficiency is inversely proportional to the collector size.

Next, let us define the product of $\Delta p_{13} A_c V_2/(q'' A_r g h_c \beta/c_p)$ as the 'Dimensionless Δp_{13} '. The reasons for this naming are that the product is dimensionless and can be interpreted as "Δp_{13} is scaled by $(q'' A_r g h_c \beta/c_p)/A_c V_2$ in the product." The characteristic of 'Dimensionless Δp_{13} ' is illustrated in Fig. 12. Although the flow properties between plants are widely scattered as displayed in Figs. 8–11, it is important to notice from Fig. 12 that the values of 'Dimensionless Δp_{13} ', are approximately equal to unity for all plants. To investigate the reason for the obtained results, let us consider the dimensionless number proposed in Ref. [26]. Reference [26] proposed that, for solar chimney power plants without a turbine work extraction,

$$\frac{\dot{m} V_2^2/2}{q'' A_r g h_c \beta/c_p} = 1. \tag{27}$$

Assuming that the whole available driving pressure is used to accelerate the air and is thus converted completely into kinetic energy, we have

$$\Delta p_{13} A_c V_2 = \dot{m} V_2^2/2. \tag{28}$$

Consequently,

$$\frac{\Delta p_{13} A_c V_2}{q'' A_r g h_c \beta/c_p} = 1 \tag{29}$$

as confirmed by Fig. 12. As a result, Eq. (29) can principally be used to evaluate the available driving pressure of solar chimney power plants.

Fig. 13 presents Δp_{loss}, the pressure difference between Δp_{13} and Δp_{23}. Surprisingly all data collapse into one single line! It is found that

$$\Delta p_{loss} = 0.0002 \dot{m}^2 \tag{30}$$

regardless of the plant size or the solar heat flux! Consequently, we can use Eqs. (29) and (30) together with the collector efficiency from Fig. 11 to approximate the turbine output power for solar chimney systems.

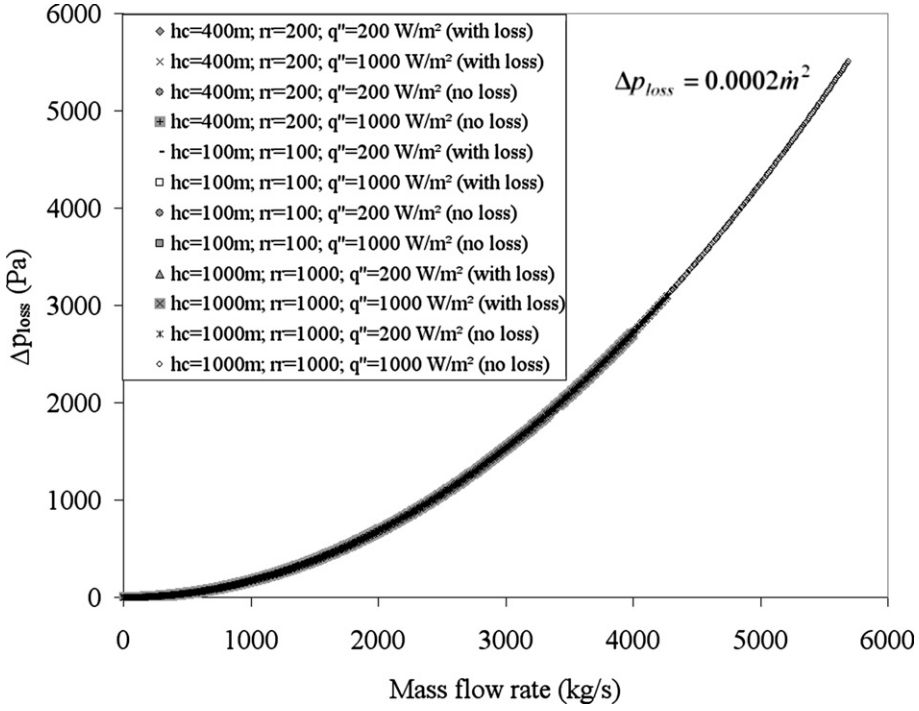

Fig. 13. Influence of mass flow rate on plant total pressure loss along lines of constant solar irradiation. ($h_r = 2$ m and $r_c = 4$ m for all plants).

6. Conclusion

Theoretical simulations were conducted in order to evaluate the performance of solar chimney power plants. The relationships between the pressure ratio and the mass flow rate and between the temperature rise across the collector and the power output were presented. It was found that, for the system with a constant driving pressure (available system pressure difference), the optimum ratio of the turbine extraction pressure to the driving pressure is 2/3. For the system with the non-constant driving pressure, it is obvious that this optimum ratio is a function of the plant size and solar heat flux. This observation would be helpful in the preliminary plant design. In addition, it was shown that the appropriate plant, which can serve the electricity demand for each village in Thailand and the investment cost would be affordable by the local government, is the one with a collector radius of 200 m and a chimney height of 400 m. The optimum pressure ratio for the proposed plant is equal to 0.84 approximately. The paper also proposes the simple method to primarily evaluate the turbine power output for solar chimney systems.

Economic viability requires the optimum configurations of each component. To develop a mathematical statement for optimization, we need a simple-but-accurate mathematical model of solar chimney power plants. Even though the solar chimney power plant concept has been proposed and intensively studied before by several different researchers. The mathematical models proposed in the literature are mathematically so complex and some of them do not in the form that suitable for us to optimize. The mathematical model presented here is relatively simple while provides a very accurate result as shown in Table 4. So we will use the present mathematical model to find the optimum operating conditions for the whole system in our next study.

Acknowledgments

This research was sponsored by the SUT Research and Development fund of Suranaree University of Technology (SUT), Thailand.

References

[1] Schlaich J. The solar chimney. Stuttgart, Germany: Edition Axel Menges; 1995.
[2] Haaf W, Friedrich K, Mayr G, Schlaich J. Solar chimneys: part I: principle and construction of the pilot plant in Manzanares. Int J Sol Energ 1983;2:3–20.
[3] Mullett LB. The solar chimney – overall efficiency, design and performance. Int J Ambient Energ 1987;8(1):35–40.
[4] Lodhi MAK. Application of helio-aero-gravity concept in producing energy and suppressing pollution. Energ Convers Manage 1999;40:407–21.
[5] Von Backström TW, Gannon AJ. The solar chimney air standard thermodynamic cycle. SAIMechE R&D J 2000;16(1):16–24.
[6] Dai YJ, Huang HB, Wang RZ. Case study of solar chimney power plants in northwestern regions of China. Renew Energ 2003;28:1295–304.
[7] Nizetic S, Ninic N, Klarin B. Analysis and feasibility of implementing solar chimney power plants in the Mediterranean region. Energy 2008;33(11):1680–90.
[8] Kashiwa BA, Kashiwa CB. The solar cyclone: a solar chimney for harvesting atmospheric water. Energy 2008;33(2):331–9.
[9] Hedderwick RA. Performance evaluation of a solar chimney power plant. M.Sc. Eng.-thesis: University of Stellenbosch, Stellenbosch, South Africa, 2001.
[10] Von Backström TW, Fluri TP. Maximum fluid power condition in solar chimney power plants – an analytical approach. Sol Energy 2006;80:1417–23.
[11] Nizetic S, Klarin B. A simplified analytical approach for evaluation of the optimal ratio of pressure drop across the turbine in solar chimney power plants. Appl Energy 2010;87(2):587–91.
[12] Schlaich J, Bergermann R, Schiel W, Weinrebe G. Design of commercial solar updraft tower systems utilization of solar induced convective flows for power generation. J Sol Energ-T ASME 2005;127:117–24.
[13] Bernardes MA, Dos S, Voß A, Weinrebe G. Thermal and technical analyses of solar chimneys. Sol Energy 2003;75(6):511–24.
[14] Pasumarthi N, Sherif SA. Experimental and theoretical performance of a demonstration solar chimney model – part I: mathematical model development. Int J Energ Res 1998;22:277–88.
[15] Pastohr H, Kornadt O, Gürlebeck K. Numerical and analytical calculations of the temperature and flow field in the upwind power plant. Int J Energ Res 2004;28:495–510.
[16] Onyango FN, Ochieng RM. The potential of solar chimney for application in rural areas of developing countries. Fuel 2006;85:2561–6.
[17] Koonsrisuk A, Lorente S, Bejan A. Constructal solar chimney configuration. Int J Heat Mass Tran 2010;53(1–3):327–33.
[18] Koonsrisuk A. Mathematical modeling of sloped solar chimney power plants. Energy, http://dx.doi.org/10.1016/j.energy.2012.09.039; 2012.
[19] Chitsomboon T. A validated analytical model for flow in solar chimney. Int J Renew Energ Eng 2001;3(2):339–46.
[20] Duffie J, Beckman WA. Solar engineering of thermal processes. 2nd ed. USA: John Wiley & Sons, Inc; 1991.
[21] Calvert JG. Glossary of atmospheric chemistry terms (Recommendations 1990). Pure Appl Chem 1990;62(11):2167–219.
[22] Zhou XP, Bernardes MA dos S, Ochieng RM. Influence of atmospheric cross flow on solar updraft tower inflow. Energy 2012;42(1):393–400.
[23] Haaf W. Solar chimneys: part II: preliminary test results from the Manzanares plant. Int J Sol Energ 1984;2:141–61.
[24] Weinrebe G, Schiel W. Up-draught solar tower and down-draught energy tower – a comparison. Proceedings of the ISES solar World Congress 2001: Adelaide, Australia, 2001.
[25] Provincial Electricity Authority of Thailand. 2007. Annual report [On-line]. Available from: http://www.pea.co.th/annualreport/2007/PEA.swf.
[26] Koonsrisuk A, Chitsomboon T. A single dimensionless variable for solar tower plant modeling. Sol Energy 2009;83(12):2136–43.

Nomenclature

A: flow area, m^2
A_r: roof area, m^2
c_p: specific heat capacity at constant pressure, J/(kg K)
g: gravitational acceleration, m/s^2
h_c: chimney height, m
h_r: roof height above the ground, m
I: solar irradiation, W/m^2
M: Mach number
$\dot{m}$: mass flow rate, kg/s
p: pressure, Pa
q'': insolation, W/m^2
R: ideal gas constant, J/kg K
r_c: chimney radius, m
r_r: roof radius, m
T: absolute temperature, K
U: collector loss coefficient, W/m^2 K
V: flow velocity, m/s
x: pressure ratio, Eq. (2)
v: specific volume, m^3/kg
W: power, W
z: cartesian coordinate in vertical direction

Greek symbols
α: collector absorption coefficient
β: coefficient of volumetric thermal expansion, 1/K
Δp: pressure drop, Pa
ΔT: temperature rise between ambient and collector outlet, K
γ: specific heat ratio
η_{col}: collector efficiency
ρ: density, kg/m^3

Subscripts
1,2,3,4: position along chimney (as depicted in Fig. 1)
c: chimney
dyn: dynamic pressure component
ext: extraction by the turbine
loss: difference between the available driving pressure and the turbine extraction pressure
no turb: without turbine
opt: optimum
r: roof
tot: total pressure component
turb: turbine
with turb: with turbine
∞: free stream